An $R_{1\rho}$ expression for a spin in chemical exchange between two sites with unequal transverse relaxation rates

Andrew J. Baldwin & Lewis E. Kay

Journal of Biomolecular NMR

ISSN 0925-2738
Volume 55
Number 2

J Biomol NMR (2013) 55:211-218
DOI 10.1007/s10858-012-9694-6

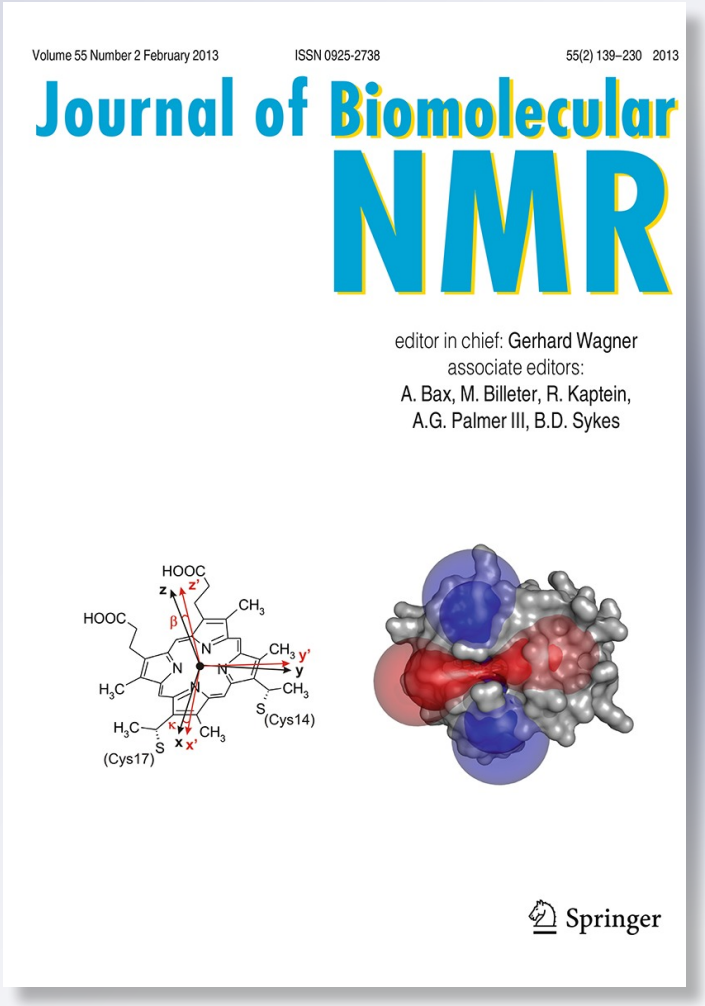

Springer

J Biomol NMR (2013) 55:211–218
DOI 10.1007/s10858-012-9694-6

ARTICLE

An $R_{1\rho}$ expression for a spin in chemical exchange between two sites with unequal transverse relaxation rates

Andrew J. Baldwin · Lewis E. Kay

Received: 14 August 2012 / Accepted: 6 December 2012 / Published online: 23 January 2013

Abstract An analytical expression is derived for the rotating frame relaxation rate, $R_{1\rho}$, of a spin exchanging between two sites with different transverse relaxation times. A number of limiting cases are examined, with the equation reducing to formulae derived previously under the assumption of equivalent relaxation rates at each site. The measurement of a pair off-resonance $R_{1\rho}$ values, with the carrier displaced equally on either side of the observed correlation, forms the basis of one of the approaches for obtaining signs of chemical shift differences, $\Delta\omega$, of exchanging nuclei. The results presented here establish that this method is relatively insensitive to differential transverse relaxation rates between the exchaning states, greatly simplifying the calculation of optimal parameters in $R_{1\rho}$ based experiments that are used for measurement of signs of $\Delta\omega$.

Keywords Relaxation dispersion NMR · Invisible excited states · Protein conformational exchange · Spin-lock · Rotating frame relaxation · Differential transverse relaxation

A. J. Baldwin (✉) · L. E. Kay
Departments of Molecular Genetics, Biochemistry and Chemistry, University of Toronto, Toronto, ON M5S 1A8, Canada
e-mail: andrew.baldwin@chem.ox.ac.uk

Present Address:
A. J. Baldwin
Physical and Theoretical Chemistry Laboratory, University of Oxford, South Parks Road, Oxford OX1 3QZ, UK

L. E. Kay
Hospital for Sick Children, Program in Molecular Structure and Function, 555 University Avenue, Toronto, ON M5G 1X8, Canada

Introduction

The structures spontaneously adopted by proteins dictate their function. The interactions that stabilize these structures are individually weak and at biologically relevant temperatures are easily rearranged by thermal motion. Consequently, biological molecules are inherently dynamic (Karplus and Kuriyan 2005) and are best understood as ensembles of interconverting conformers rather than in terms of single static structures (Lange et al. 2008; Lindorff-Larsen et al. 2005). Moreover, it is increasingly apparent that conformational fluctuations play crucial roles in enabling the functions of protein molecules (Karplus and Kuriyan 2005). Observing and characterizing such motions however remains challenging.

Solution NMR spectroscopy is particularly well suited to characterizing such molecular dynamics over a broad spectrum of time-scales (Ishima and Torchia 2000; Mittermaier and Kay 2006; Palmer et al. 1996). Among the different methodologies, paramagnetic relaxation enhancement (Iwahara and Clore 2006), $R_{1\rho}$ (Palmer and Massi 2006) and Carr-Purcell-Meiboom-Gill (CPMG) (Hansen et al. 2008; Korzhnev and Kay 2008; Palmer et al. 2001) experiments are particularly useful for the study of exchange processes involving the inter-conversion between dominant (ground) and sparsely populated (conformationally 'excited') states. Insight into biological processes as diverse as molecular recognition, ligand binding, enzyme catalysis and protein folding, has been achieved using these techniques (Boehr et al. 2006; Fraser et al. 2009; Henzler-Wildman and Kern 2007; Ishima et al. 1999; Korzhnev et al. 2004, 2010; Sugase et al. 2007; Tang et al. 2007).

A rich theoretical basis for understanding PRE, $R_{1\rho}$ and CPMG-based experiments as they pertain to systems undergoing chemical exchange has emerged over many years. Notably, analytical expressions exist that describe the

effective $R_{1\rho}$ or R_2 relaxation rate as a function of the exchange parameters, radio frequency (RF) field strengths and shift offsets (Allerhand et al. 1966; Carver and Richards 1972; Deverell et al. 1970; Jen 1978; Luz and Meiboom 1963; Miloushev and Palmer 2005; Palmer et al. 2001, 2005; Palmer and Massi 2006; Trott and Palmer 2002). While explicit use of these equations in fits of experimental data has now given way to numerical approaches involving fast computers, analytical expressions remain useful for providing physical insight that various parameters have on the measured relaxation rates. Most recently, Palmer and coworkers and Ishima and Torchia have derived analytical expressions for CPMG and $R_{1\rho}$ experiments that extend the relations that were originally presented many years ago (Ishima and Torchia 1999; Miloushev and Palmer 2005; Trott and Palmer 2002).

The majority of the derived formulae for transverse relaxation in the presence of CPMG or $R_{1\rho}$ fields are based on the assumption that the spins in question exchange between states with the same intrinsic transverse relaxation rates, $\Delta R_2 = 0$, although Allerhand and Thiele recognized very early on that large differences in transverse relaxation rates of exchanging spins can certainly influence the CPMG profile (Allerhand and Thiele 1966). More recently, Ishima and Torchia have explored through simulations how CPMG dispersion profiles are affected in the case where $\Delta R_2 \neq 0$ (Ishima and Torchia 2006). In addition, Miloushev and Palmer have presented an expression to account for relaxation differences in $R_{1\rho}$ experiments that is valid in certain limits (Miloushev and Palmer 2005). There are clearly many cases where the assumption $\Delta R_2 = 0$ is reasonable. However, recent advances in NMR methodology have opened the possibilities of studying biological molecules of ever-increasing size (Fiaux et al. 2002; Sprangers and Kay 2007), leading to examples where differential relaxation becomes an important issue. This is the case for the 560 kDa αB-crystallin oligomeric ensemble (Baldwin et al. 2011a, b), where we have recently characterized a disorder (ground state) to order (excited state) transition with $\Delta R_2 \sim 200\ s^{-1}$ (Baldwin et al. 2012), illustrated schematically in Fig. 1. In an effort to understand how such differences affect measured $R_{1\rho}$ relaxation rates we have derived an expression for $R_{1\rho}$ in the limit $\Delta R_2 \neq 0$ that is valid over a large range of ΔR_2 values (see below). We show that differential transverse relaxation can significantly influence $R_{1\rho}$ rates but that remarkably measurements of signs of chemical shift differences, based on comparison of $R_{1\rho}$ values obtained with spinlock fields on either sides of the ground state correlation (Korzhnev et al. 2003; Trott and Palmer 2002), are much less affected by $\Delta R_2 \neq 0$.

Results and discussion

We consider here the case of two-site conformational exchange involving the interconversion of a molecule between ground (G) and excited (E) states, $G \underset{k_{EG}}{\overset{k_{GE}}{\rightleftarrows}} E$ and focus on a single spin reporter. In what follows, the fractional populations of the two states are given by $p_G = k_{EG}/k_{ex}$ and $p_E = 1 - p_G = k_{GE}/k_{ex}$, the overall exchange rate is $k_{ex} = k_{EG} + k_{GE}$, the spin of interest in each of the two states evolves with frequencies ω_G and ω_E ($\Delta\omega = \omega_E - \omega_G$, rad/s) in the absence of chemical exchange and the difference in intrinsic transverse spin relaxation rates is given by ΔR_2. As has been described in the literature (Anet and Basus 1978; Skrynnikov et al. 2002), chemical exchange leads to a shift in the position of the observed resonance from ω_G to ω_{OBS} where in the limit that $p_G \gg p_E$,

$$\omega_{ex} = \omega_{OBS} - \omega_G = \frac{k_{EG}k_{GE}\Delta\omega}{(k_{EG} + \Delta R_2)^2 + (\Delta\omega)^2}. \quad (1)$$

In a typical $R_{1\rho}$ experiment that is of interest here, magnetization initially along the z-axis is rotated into the x–z plane by a pulse along the y axis with flip angle $\theta_{flip} = \tan^{-1}(\omega_1/\delta_{OBS})$, $\delta_{OBS} = \omega_{OBS} - \omega_{RF}$ where ω_{RF} is the carrier frequency. The resulting spin-locked magnetization subsequently evolves for a defined period of time under the influence of an RF pulse of strength ω_1 applied along the x-axis at an offset of δ_{OBS} from the observed ground state frequency. At the completion of this interval magnetization is subsequently restored to the z-axis by a y pulse with flip angle $-\theta_{flip}$. The decay rate of the signal, $R_{1\rho}$ can be analyzed to determine the properties of the underlying conformational exchange (Palmer and Massi 2006). The evolution of

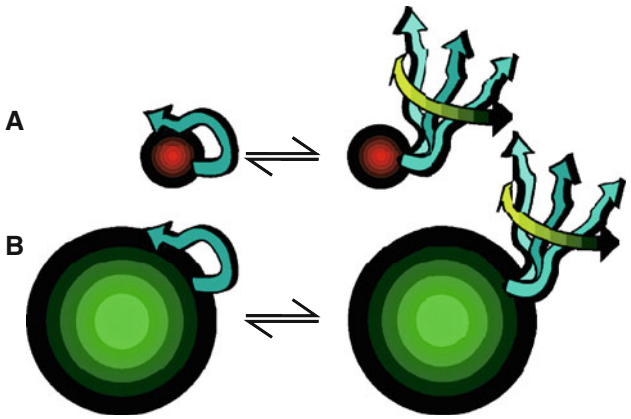

Fig. 1 Schematic of a two-site exchange process involving the interconversion between protein conformers whereby a fragment is rigidly bound or unattached to the core of the protein. In the case where the protein is small (molecular mass of 5–10 kDa, **a**) it may be that differential transverse relaxation in the two states can be neglected in the analysis of exchange data (although this must be rigorously established). In the case of a high molecular weight complex, such as αB crystallin (aggregate molecular mass of close to 600 kDa, illustrated schematically in **b**) ΔR_2 can be large ($\approx 200\ s^{-1}$), complicating analysis of dispersion data

magnetization during the spin-lock period is given by a set of coupled linear differential equations (McConnell 1958),

$$\frac{d}{dt}\begin{pmatrix} M_x^G \\ M_y^G \\ M_z^G \\ M_x^E \\ M_y^E \\ M_z^E \end{pmatrix} = \begin{pmatrix} -R_2^G - k_{GE} & -\delta_G & 0 & k_{EG} & 0 & 0 \\ \delta_G & -R_2^G - k_{GE} & -\omega_1 & 0 & k_{EG} & 0 \\ 0 & \omega_1 & -R_1^G - k_{GE} & 0 & 0 & k_{EG} \\ k_{GE} & 0 & 0 & -R_2^E - k_{EG} & -\delta_G - \Delta\omega & 0 \\ 0 & k_{GE} & 0 & \delta_G + \Delta\omega & -R_2^E - k_{EG} & -\omega_1 \\ 0 & 0 & k_{GE} & 0 & \omega_1 & -R_1^E - k_{EG} \end{pmatrix} \begin{pmatrix} M_x^G \\ M_y^G \\ M_z^G \\ M_x^E \\ M_y^E \\ M_z^E \end{pmatrix} + \overrightarrow{M_0} \qquad (2)$$

where $\vec{M}_O = \left(0, 0, R_1^G M_O^G, 0, 0, R_1^E M_O^E\right)^T$, T is 'transpose', $R_1^{G/E}$ and $R_2^{G/E}$ are longitudinal and transverse relaxation rates for the spin in states G, E and $M_0^{G/E}$ are thermal equilibrium magnetization values, proportional to p_G and p_E. In what follows we assume $R_1^E = R_1^G = R_1$ and $R_2^E \neq R_2^G$. Note that the assumption of equivalent R_1 values is reasonable even if states G and E differ significantly in correlation time or in intrinsic dynamics since R_1 rates are in general small for the spin ½ probes of dynamics typically used in studies of biomolecules.

Following the lead of Trott and Palmer (2002) an expression for the $R_{1\rho}$ rate when $R_2^E \neq R_2^G$ is derived by evaluating,

$$\det\left|\hat{R} - \lambda\hat{E}\right| = 0 \qquad (3)$$

where $\hat{E}$ is the identity matrix and $\hat{R}$ is the 6×6 square matrix in Eq. (2). Of the six eigenvalues of $\hat{R}$, four are complex, and of the two that are real only one is small in magnitude, corresponding to the $R_{1\rho}$ value measured experimentally (Trott and Palmer 2002). Evaluating the characteristic polynomial that derives from Eq. (3), with the substitutions $\Delta R_2 = R_2^E - R_2^G$ and $\Delta R = R_2^G - R_1$ generates 230 non-zero terms of the form $C(\Delta\omega)^i \delta_G^j \omega_1^k k_{EG}^l k_{GE}^m (\Delta R)^n (\Delta R_2)^o \lambda^p$ where C is a number and the sum of all superscripts is equal to 6. In general it is not possible to obtain an analytical solution for the roots (eigenvalues) of a polynomial of order 6, however, as discussed by Trott and Palmer (2002) only the leading terms of the polynomial must be retained to calculate an accurate expression for $R_{1\rho}$. Because in many practical cases both the eigenvalue of interest (λ, corresponding to $-R_{1\rho}$) and ΔR are small compared to the other elements in each of the 230 terms ($\Delta\omega$, δ_G, ω_1, k_{EG}, k_{GE}, ΔR_2) it is possible to include only those terms in the characteristic polynomial for which $n + p \leq 1$ without unduly sacrificing accuracy. This follows directly from the fact that for higher powers of ΔR and λ the terms become small. The linear (in λ) equation that results, $A\lambda + B = 0$, contains 76 terms, with $\lambda = -B/A = -R_{1\rho}$.

After a lengthy derivation, and with the following definitions,

$$\begin{aligned} \delta_j &= \omega_j - \omega_{RF}, \quad j \in \{G, E\} \\ \overline{\delta} &= p_G\delta_G + p_E\delta_E = \delta_G + p_E\Delta\omega \\ \Omega_G^2 &= \omega_1^2 + \delta_G^2 \\ \Omega_E^2 &= \omega_1^2 + \delta_E^2 \\ \overline{\Omega}^2 &= \omega_1^2 + \overline{\delta}^2 \\ \theta &= \tan^{-1}\left(\omega_1/\overline{\delta}\right) \end{aligned} \qquad (4)$$

we arrive at the central result of the paper,

$$R_{1\rho} = C_{R1}R_1\cos^2\theta + \left(C_{R2}R_2^G + R_{2ex}\right)\sin^2\theta \qquad (5)$$

where $\sin^2\theta = \omega_1^2/\overline{\Omega}^2$ and $\cos^2\theta = \overline{\delta}^2/\overline{\Omega}^2$. Note that $\theta = \theta_{flip}$ only in the limit $\omega_G + p_E\Delta\omega \approx \omega_{OBS}$. The coefficients C_{R1}, C_{R2} and R_{2ex} include explicit contributions from ΔR_2 and are given by

$$\begin{aligned} C_{R1} &= \frac{F_2^P + \left(F_1^P + \Delta R_2(F_3 - F_2)\right)\tan^2\theta}{D^P + \Delta R_2 F_3 \sin^2\theta} \\ C_{R2} &= \frac{\left(D^P\csc^2\theta - F_2^P\cot^2\theta\right) - F_1^P + \Delta R_2 F_2}{D^P + \Delta R_2 F_3 \sin^2\theta} \\ R_{2ex} &= \frac{F_1^P k_{ex} + \Delta R_2 F_1}{D^P + \Delta R_2 F_3 \sin^2\theta} \end{aligned} \qquad (6)$$

These are, in turn, recast in terms of three expressions that are independent of ΔR_2, present in the derivation by Trott and Palmer (2002),

$$\begin{aligned} F_1^P &= p_G p_E \Delta\omega^2 \\ F_2^P &= k_{ex}^2 + \omega_1^2 + \frac{\delta_G^2\delta_E^2}{\overline{\delta}^2} \\ D^P &= k_{ex}^2 + \frac{\Omega_G^2\Omega_E^2}{\overline{\Omega}^2} \end{aligned} \qquad (7)$$

and an additional three terms that are all multiplied by ΔR_2 in C_{R1},C_{R2} and R_{2ex},

$$F_1 = p_E\left(\Omega_G^2 + k_{ex}^2 + \Delta R_2 p_G k_{ex}\right)$$
$$F_2 = 2k_{ex} + \frac{\omega_1^2}{k_{ex}} + \Delta R_2 p_G$$
$$F_3 = 3p_E k_{ex} + \left(2p_G k_{ex} + \frac{\omega_1^2}{k_{ex}} + \Delta R_2 + \frac{\Delta R_2 p_E^2 k_{ex}^2}{\Omega_G^2}\right)\left(\frac{\Omega_G^2}{\omega_1^2}\right) \quad (8)$$

Equation (5) is complicated and it is useful to consider certain limiting cases. Assuming for the moment that $\Delta R_2 = 0$ it is straightforward to show that

$$R_{1\rho} = R_2 + \frac{\left(k_{ex}^2 + \omega_1^2 + \frac{\delta_G^2\delta_E^2}{\delta^2}\right)(R_1 - R_2)\cos^2\theta + p_G p_E \Delta\omega^2 (k_{ex} + R_1 - R_2)\sin^2\theta}{k_{ex}^2 + \frac{\Omega_G^2\Omega_E^2}{\Omega^2}} \quad (9)$$

$(R_2^E = R_2^G = R_2)$ which is identical to Eq. (11) of Trott and Palmer (2002) (not withstanding a small typographical error in their expression). In the limit that $\Delta R/k_{ex} \ll 1$ and $\delta_G \gg p_E \Delta\omega$ it follows that

$$R_{1\rho}^P = R_1 \cos^2\theta + (R_2 + R_{ex}^P)\sin^2\theta \quad (10)$$

where

$$R_{ex}^P = \frac{p_G p_E \Delta\omega^2 k_{ex}}{\frac{\Omega_E^2\Omega_G^2}{\Omega^2} + k_{ex}^2} \cong \frac{p_G p_E \Delta\omega^2 k_{ex}}{\Omega_E^2 + k_{ex}^2}, \quad (11)$$

that is Eq. (21) of Trott and Palmer (2002).

Equation (5) can be simplified in the limit when ΔR_2 is small by performing a Taylors series expansion about $\Delta R_2 = 0$, retaining only the linear terms and enforcing $\delta_G \gg p_E \Delta\omega$, $p_G \gg p_E$. It can be shown that under these conditions

$$C_{R1}^{\Delta R_2 \to 0} = 1 + \frac{p_E \Delta\omega^2}{k_{ex}^2 + \Omega_E^2}\tan^2\theta + \frac{\Delta R_2 \Xi}{k_{ex}^2 + \Omega_E^2}\tan^2\theta$$
$$C_{R2}^{\Delta R_2 \to 0} = 1 - \frac{p_E \Delta\omega^2}{k_{ex}^2 + \Omega_E^2} - \frac{\Delta R_2 \Xi}{k_{ex}^2 + \Omega_E^2}$$
$$R_{2ex}^{\Delta R_2 \to 0} = \frac{p_E \Delta\omega^2 k_{ex}}{k_{ex}^2 + \Omega_E^2}\left(1 + \frac{\Delta R_2}{k_{ex}}\left(\frac{k_{ex}^2 + \Omega_G^2}{\Delta\omega^2} - \frac{2k_{ex}^2 + \omega_1^2}{k_{ex}^2 + \Omega_E^2}\right)\right) \quad (12)$$
$$\Xi = p_E\left(\left(1 - 3\cos^2\theta\right)k_{ex} - \left(\frac{2k_{ex}^2 + \omega_1^2}{k_{ex}^2 + \Omega_E^2}\right)\left(\frac{\Delta\omega^2}{k_{ex}}\right)\right)$$

Substitution of the expressions in Eq. (12) into Eq. (5) with the requirement that $\Delta R/k_{ex} \ll 1$ and retaining only the leading terms gives

$$R_{1\rho}^{\Delta R_2 \to 0} = R_1 \cos^2\theta + \left(R_2^G + R_{2ex}^{\Delta R_2 \to 0}\right)\sin^2\theta. \quad (13)$$

From the expression for $R_{2ex}^{\Delta R_2 \to 0}$ in Eq. (12) it is clear that so long as

$$\frac{\Delta R_2}{k_{ex}} << \left|\frac{\Delta\omega^2\left(k_{ex}^2 + \Omega_E^2\right)}{\left(k_{ex}^2 + \Omega_G^2\right)\left(k_{ex}^2 + \Omega_E^2\right) - \left(2k_{ex}^2 + \omega_1^2\right)\Delta\omega^2}\right| \quad (14)$$

differential transverse relaxation makes little contribution to $R_{1\rho}$, while as k_{ex} increases the effects of ΔR_2 become more pronounced (see below).

Values of $R_{1\rho}$ as a function of ω_1 have been calculated with (i) Eq. (11) of Trott and Palmer (2002), modified as they describe with R_1 and R_2 in this expression replaced by population weighted averages, (ii) with Eq. (5) or (iii) numerically for exchange parameters indicated in the legend to Fig. 2a, b. When $\Delta R_2 = 0$ (Fig. 2a) excellent agreement is obtained with the numerically computed values. The slight deviations observed for small ω_1 values are in keeping with the assumptions used in the derivation of analytical expressions based on linearization of the characteristic polynomial of the matrix in Eq. (2). Significant deviations are noted for the Trott and Palmer expression when ΔR_2 is large ($R_2^G = 6\ s^{-1}$, $R_2^E = 200\ s^{-1}$), as expected, while rates calculated with Eq. (5) are in good agreement with those obtained numerically, Fig. 2b. These differences decrease as ω_1 increases but do not go to zero in the present case as this would require in addition that $\Delta R_2/k_{ex} \ll 1$, a condition that is not fulfilled in this example (see legend to Fig. 2). Of note, similar calculations, but as a function of k_{ex}, show that the differences between the expressions do converge to the exchange free rate in the tilted frame in the limit that $k_{ex} \to \infty$ with R_1 and R_2 values given by population weighted averages. We have also performed an extensive grid search in parameter space to ascertain the accuracy of Eq. (5) more generally. Numerical simulations for $R_2^G \le R_2^E \le 500 s^{-1}$, $0.1\ \% \le p_E \le 10\ \%$, $12.5\ rad/s \le \Delta\omega \le 12{,}500\ rad/s$, $10\ s^{-1} \le k_{ex} \le 20{,}000\ s^{-1}$, $25\ rad/s \le \omega_1 \le 100{,}000\ rad/s$, $0.001\ rad/s \le \delta_G \le 100{,}000\ rad/s$ show that, so long as $(\delta_G^2 + \omega_1^2)^{0.5} > A(p_E\Delta\omega)^2$ with $A = 0.1$, errors are less than $2\ s^{-1}$. Figure 2c plots the deviations in $R_{1\rho}$ values calculated from Eq. (5) or from the formula of Trott and Palmer for a number of R_2^E values as a function of A. As the value

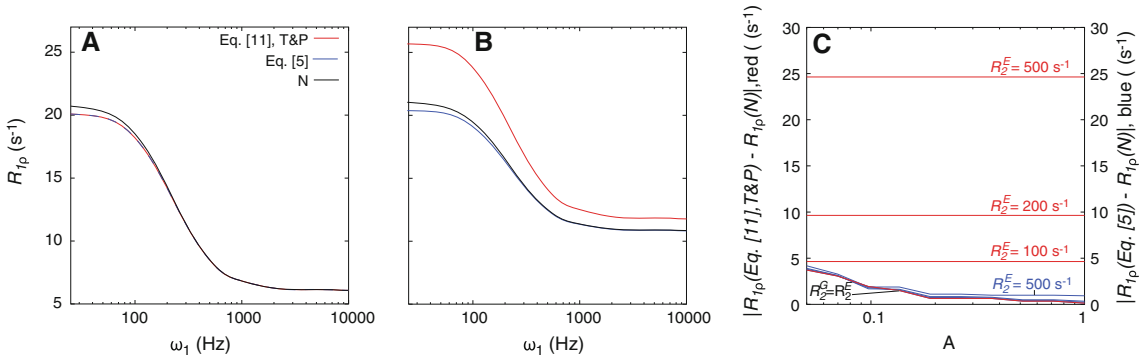

Fig. 2 **a**, **b** Plots of $R_{1\rho}(\omega_1)$ calculated with (*i*) Eq. (11) of Trott and Palmer (2002), modified such that R_1 and R_2 in this expression are replaced by population weighted averages (*red*), (*ii*) with Eq. (5) of the present manuscript (*blue*) and (*iii*) by solving numerically for $R_{1\rho}$ using Eq. (2) (*black*) for $\Delta R_2 = 0$ (**a**) and $R_2^G = 6\,s^{-1}$, $R_2^E = 200 s^{-1}$ (**b**). Values of $k_{ex} = 1{,}000\ s^{-1}$, $\Delta\omega = 1{,}000$ rad/s, $R_1 = 2.5\ s^{-1}$, $\delta_G = 0$ rad/s, $p_B = 3$ % have been used. In the limit $\omega_1 \rightarrow \infty$ Eq. (5) reduces to $R_{1\rho} = R_2^G + \frac{\Delta R_2 p_E}{1+\Delta R_2/k_{ex}}$ that differs slightly from a population weighted average of rates, $p_G R_2^G + p_E R_2^E$. Note that an identical expression is obtained in this limit for the transverse relaxation rate derived from the CPMG experiment as well. **c** Errors in $R_{1\rho}$ values calculated from Eq. (5) [*blue*, $R_{1\rho}$(Eq. (5))] or Eq. (11) of Trott and Palmer [*red*, $R_{1\rho}$(Eq. (11), T&P)] for $R_2^E = (6, 100, 200, 500\,s^{-1})$ as a function of A, with $(\delta_G^2 + \omega_1^2)^{0.5} > A(p_E\Delta\omega)^2$ and spanning the range $R_2^G \le R_2^E \le 500\,s^{-1}$, 0.1 % $\le p_E \le$ 10 %, 12.5 rad/s $\le \Delta\omega \le$ 12,500 rad/s, $10\ s^{-1} \le k_{ex} \le 20{,}000\ s^{-1}$, 25 rad/s $\le \omega_1 \le$ 100,000 rad/s, 0.001 rad/s $\le \delta_G \le$ 100,000 rad/s. For $A = 0.1$ errors are less than 2 s^{-1} using Eq. (5). Values of $R_{1\rho}$ calculated by numerically computing the eigenvalues of the matrix in Eq. (3) are denoted by $R_{1\rho}(N)$

of A decreases in the expression above the range of possible δ_G, ω_1 values increases, leading to cases where $R_{1\rho}$ becomes sufficiently large that retaining only those terms up to linear in λ in the polynomial of Eq. (3) is no longer appropriate so that Eq. (5) becomes less accurate.

As an interesting application of the work described here we consider the measurement of $R_{1\rho}$ as a function of offset from the ground state peak to obtain the sign of $\Delta\omega$, and hence the value for the resonance position of the spin in the excited conformer. This information is not available from Carr-Purcell-Meiboom-Gill experiments that are typically recorded to characterize exchanging systems since relaxation dispersion profiles are only sensitive to $|\Delta\omega|$. In their original derivation of an expression for $R_{1\rho}$ outside the fast exchange regime Trott and Palmer (2002) noted that $R_{1\rho}$ values are particularly sensitive to the placement of the spin lock field relative to the resonance frequency in the ground state, with a maximum in R_{2ex} when the carrier is positioned on resonance with the peak derived from the excited state. Thus, $R_{1\rho}(\delta_G = \Delta\omega) < R_{1\rho}(\delta_G = -\Delta\omega)$. Our laboratory has exploited this result by measuring $R_{1\rho}$ values where the spin lock is placed equidistantly upfield and downfield of the major state correlation in a pair of experiments. Positions of the carrier and the magnitude of the spinlock field (ω_1) are optimized on a per-residue basis, taking into account the exchange parameters that have been measured previously, by maximizing the difference in $R_{1\rho}$ values for a given spin lock duration, T_{relax}. Using this approach we have developed a suite of off-resonance $R_{1\rho}$ experiments with weak spinlock fields to measure the signs of chemical shift differences for $^1H^\alpha$, $^1H^N$, ^{15}N, $^{13}C^\alpha$ and ^{13}C-methyl nuclei in proteins that exchange between different conformations on the ms timescale (Auer et al. 2009, 2010; Baldwin and Kay 2012; Korzhnev et al. 2003, 2005).

Equations (12) and (13) presented above can be used to derive an expression for the difference in $R_{1\rho}$ relaxation rates recorded with the spinlock carrier placed downfield ($R_{1\rho}^+$) and upfield ($R_{1\rho}^-$) of the ground state resonance position, $\Delta R_{1\rho} = R_{1\rho}^+ - R_{1\rho}^-$, that forms the basis for measurement of the signs of chemical shift differences. Under the same set of assumptions that were used in the derivation of Eq. (12) it can be shown that

$$\Delta R_{1\rho}^{\Delta R_2 \rightarrow 0} = \frac{4p_E|\delta_{OPT}|\Delta\omega^3 k_{ex}\sin^2\theta}{\left(k_{ex}^2+\Omega_{OPT}^2+\Delta\omega^2\right)^2-4\delta_{OPT}^2\Delta\omega^2}\left(1-\frac{\Delta R_2}{k_{ex}}\left(\frac{2\left(k_{ex}^2+\Omega_{OPT}^2+\Delta\omega^2\right)\left(2k_{ex}^2+\omega_1^2\right)}{\left(k_{ex}^2+\Omega_{OPT}^2+\Delta\omega^2\right)^2-4\delta_{OPT}^2\Delta\omega^2}-\frac{\left(\Omega_{OPT}^2+k_{ex}^2\right)}{\Delta\omega^2}\right)\right) \quad (15)$$

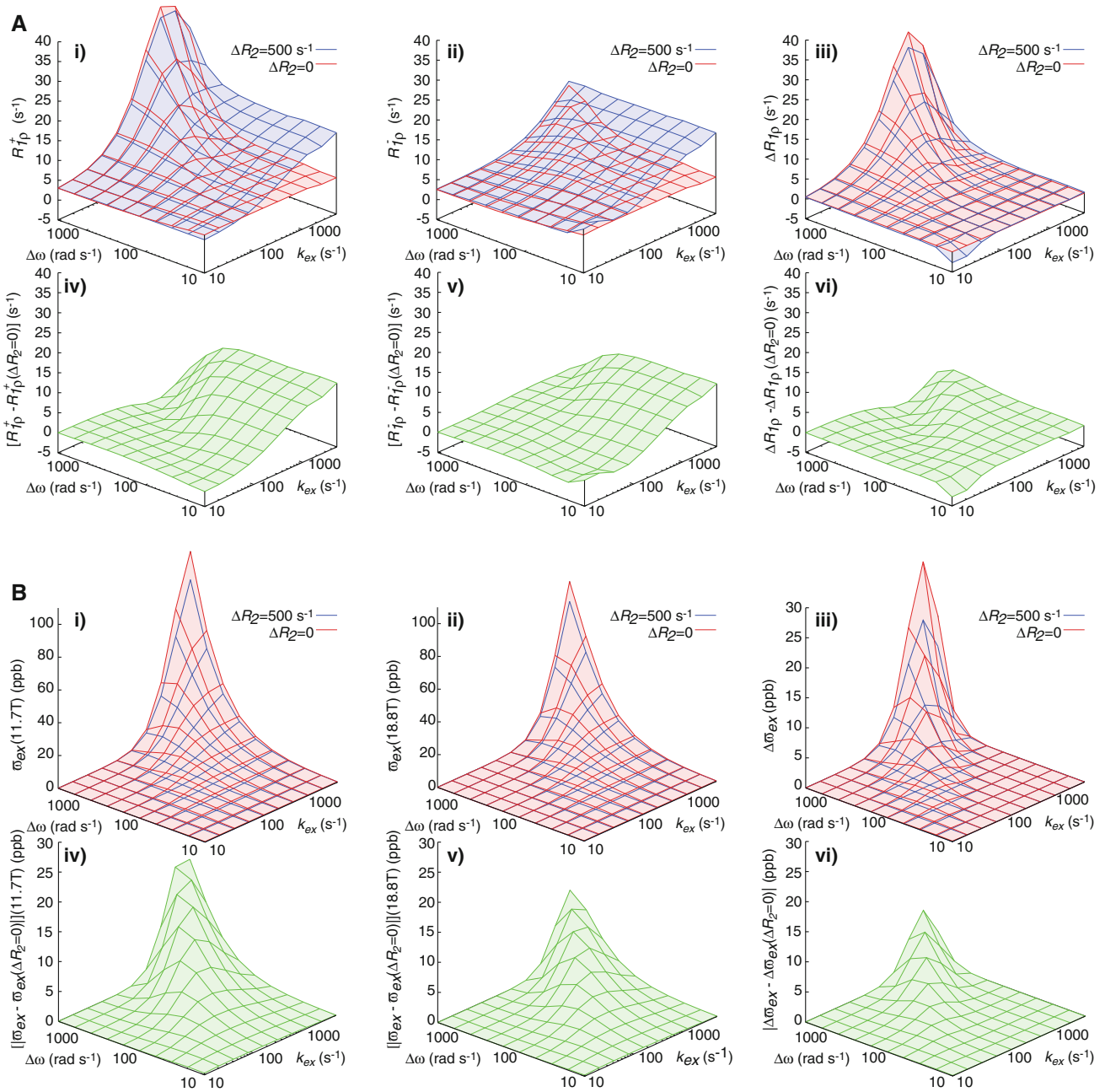

Fig. 3 **a** Plots of $R_{1\rho}^{+}$ (*i*), $R_{1\rho}^{-}$ (*ii*) and $\Delta R_{1\rho}$ (*iii*) calculated numerically, as a function of $\Delta\omega$ and k_{ex}, with $\Delta R_2 = 500\ s^{-1}$ (*blue*) or 0 (*red*). (*iv–vi*) Corresponding differences, $Z(\Delta R_2 = 500\ s^{-1}) - Z(\Delta R_2 = 0\ s^{-1})$, where $Z \in \{R_{1\rho}^{+}, R_{1\rho}^{-}, \Delta R_{1\rho}\}$, as labelled along the vertical axes. **b** (*i–iii*) Exchange induced frequency shifts (ppm), $\varpi_{ex}(\Delta\omega, k_{ex})$, calculated for static magnetic fields of 11.7 and 18.8T along with $\Delta\varpi_{ex} = \varpi_{ex}(11.7T) - \varpi_{ex}(18.8T)$, $\Delta R_2 = 500\ s^{-1}$ (*blue*) and $\Delta R_2 = 0\ s^{-1}$ (*red*). (*iv–vi*) $|\varpi_{ex}(\Delta R_2 = 500\ s^{-1}) - \varpi_{ex}(\Delta R_2 = 0\ s^{-1})|$ at 11.7T (*iv*) and 18.8T (*v*), $|\Delta\varpi_{ex}(\Delta R_2 = 500\ s^{-1}) - \Delta\varpi_{ex}(\Delta R_2 = 0\ s^{-1})|$ (*vi*)

where

$$\delta_{OPT} = \omega_{OBS} - \omega_{RF,OPT} \approx \omega_G - \omega_{RF,OPT}$$
$$\Omega_{OPT}^2 = \omega_{1,OPT}^2 + \delta_{OPT}^2 \qquad (16)$$

and $\omega_{RF,OPT}$, $\omega_{1,OPT}$ are the optimized position of the carrier and spinlock field strength, respectively.

From Eq. (15) it is clear that the sign of $\Delta\omega$ determines the sign of $\Delta R_{1\rho}$, as expected from the work of Trott and Palmer (2002); note that it can be proved that the sign of the denominator of the first term is >0 and extensive numerical simulations establish that even for ΔR_2 values as large as 500 s^{-1} the signs of $\Delta R_{1\rho}$ and $\Delta\omega$ are the same. Thus, measurement of the sign of $\Delta R_{1\rho}$ allows the determination of

the sign of $\Delta\omega$ and for positive (negative) values of $\Delta R_{1\rho}$ the excited state peak is downfield (upfield) of the ground state correlation. It is not immediately transparent from Eq. (15) how $\Delta R_2 \neq 0$ influences this scenario; however because ΔR_2 is multiplied by an expression that is, in turn, given by the difference of two positive terms there is the possibility for attenuation of the effects of differential relaxation. Indeed, this turns out to be the case, as numerical simulations indicate. Figure 3ai–iii plot $R_{1\rho}^{+}$ (i), $R_{1\rho}^{-}$ (ii) and $\Delta R_{1\rho}$ (iii) calculated from Eq. (2) numerically, as a function of $\Delta\omega$ and k_{ex} for a spin exchanging between two states with $\Delta R_2 = 500\ s^{-1}$ (blue) or 0 (red). Shown in Fig. 3aiv–vi are the differences between each of these values, $Z(\Delta R_2 = 500\ s^{-1}) - Z(\Delta R_2 = 0\ s^{-1})$, where $Z \in \{R_{1\rho}^{+}, R_{1\rho}^{-}, \Delta R_{1\rho}\}$, as labelled along the vertical axis of each panel. Most notably, $\Delta R_{1\rho}$ is rather insensitive to ΔR_2, even for very large values. Similar plots for the exchange induced frequency shift (ppm), that can also be used to establish the sign of $\Delta\omega$ (Skrynnikov et al. 2002), are shown in Fig. 3bi–iii. Here $\varpi_{ex}(\Delta\omega, k_{ex})$ values evaluated at 11.7 and 18.8T are shown, along with the difference, $\Delta\varpi_{ex} = \varpi_{ex}(11.7T) - \varpi_{ex}(18.8T)$ for both $\Delta R_2 = 500\ s^{-1}$ (blue) and $\Delta R_2 = 0\ s^{-1}$ (red). In addition absolute values of the differences between $\varpi_{ex} = \varpi_{ex}(\Delta R_2 = 500\ s^{-1})$ and $\varpi_{ex}(\Delta R_2 = 0)$ are plotted in Fig. 3biv (11.7T) and 3Bv (18.8T), respectively, along with $|\Delta\varpi_{ex}(\Delta R_2 = 500\ s^{-1}) - \Delta\varpi_{ex}(\Delta R_2 = 0)|$ in Fig. 3bvi. Values of $\Delta\varpi_{ex}$ are significantly more sensitive to ΔR_2 than are $\Delta R_{1\rho}$ rates, as indicated in the Figure. Indeed, in a previous application involving studies of chemical exchange in the 560 kDa αB crystallin complex we noted that $\Delta\varpi_{ex}$ values were much smaller than anticipated based on the measured exchange parameters, while large $\Delta R_{1\rho}$ values were still obtained from which signs of chemical shift differences could be established (Baldwin and Kay 2012).

In summary, we have derived an expression for $R_{1\rho}$ for a spin exchanging between two sites with $\Delta R_2 \neq 0$. While analytical expressions of the sort presented here can be used for data fitting we much prefer to use (exact) numerical approaches that start from the Bloch-McConnell equations. Nevertheless, formula are valuable as a 'teaching tool' providing physical insight into how the range of exchange parameters can influence measured relaxation rates. The work described here adds to a growing body of theoretical analyses of CPMG and $R_{1\rho}$ dispersion experiments and considers the important case of differential transverse relaxation that will become increasingly relevant as applications to high molecular weight biomolecules become more common.

Acknowledgments A.J.B. acknowledges the Canadian Institutes of Health Research (CIHR) for a postdoctoral fellowship and the BBSRC and Merton College for David Phillips and Fitzjames fellowships respectively. This work was supported by grants from the CIHR and the Natural Sciences and Engineering Research Council of Canada. L.E.K. holds a Canada Research Chair in Biochemistry.

References

Allerhand A, Thiele E (1966) Analysis of Carr-Prucell spinecho NMR experiments on multiple spin systems. II. The effect of chemical exchange. J Chem Phys 45:902–916

Allerhand A, Gutowsky HS, Jonas J, Meinzer RA (1966) Nuclear magnetic resonance methods for determining chemical-exchange rates. J Am Chem Soc 88:3185–3194

Anet FA, Basus VJ (1978) Limiting equations for exchanging broadening in 2-site NMR systems with very unequal populations. J Magn Reson 32:339–343

Auer R, Neudecker P, Muhandiram DR, Lundstrom P, Hansen DF, Konrat R, Kay LE (2009) Measuring the signs of 1H(alpha) chemical shift differences between ground and excited protein states by off-resonance spin-lock R(1rho) NMR spectroscopy. J Am Chem Soc 131:10832–10833

Auer R, Hansen DF, Neudecker P, Korzhnev DM, Muhandiram DR, Konrat R, Kay LE (2010) Measurement of signs of chemical shift differences between ground and excited protein states: a comparison between H(S/M)QC and R1rho methods. J Biomol NMR 46:205–216

Baldwin AJ, Kay LE (2012) Measurement of the signs of methyl 13C chemical shift differences between interconverting ground and excited protein states by R1rho: an application to aB crystallin. J Biomol NMR 53:1–12

Baldwin AJ, Hilton GR, Lioe H, Bagneris C, Benesch JL, Kay LE (2011a) Quaternary dynamics of alpha B-crystallin as a direct consequence of localised tertiary fluctuations in the C-terminus. J Mol Biol 413:310–320

Baldwin AJ, Lioe H, Robinson CV, Kay LE, Benesch JL (2011b) AlphaB-crystallin polydispersity is a consequence of unbiased quaternary dynamics. J Mol Biol 413:297–309

Baldwin AJ, Walsh P, Hansen DF, Hilton GR, Benesch JL, Sharpe S, Kay LE (2012) Probing dynamic conformations of the high molecular weight aB-crystallin heat shock protein ensemble by NMR spectroscopy. J Am Chem Soc 134:15343–15350

Boehr DD, McElheny D, Dyson HJ, Wright PE (2006) The dynamic energy landscape of dihydrofolate reductase catalysis. Science 313:1638–1642

Carver JP, Richards RE (1972) A general two-site solution for the chemical exchange produced dependence of T2 upon the Carr-Purcell pulse separation. J Magn Reson 6:89–105

Deverell C, Morgan RE, Strange JH (1970) Studies of chemical exchange by nuclear magnetic relaxation in the rotating frame. Mol Phys 18:553–559

Fiaux J, Bertelsen EB, Horwich AL, Wüthrich K (2002) NMR analysis of a 900K GroEL GroES complex. Nature 418:207–211

Fraser JS, Clarkson MW, Degnan SC, Erion R, Kern D, Alber T (2009) Hidden alternative structures of proline isomerase essential for catalysis. Nature 462:669–673

Hansen DF, Vallurupalli P, Kay LE (2008) Using relaxation dispersion NMR spectroscopy to determine structures of excited, invisible protein states. J Biomol NMR 41:113–120

Henzler-Wildman K, Kern D (2007) Dynamic personalities of proteins. Nature 450:964–972

Ishima R, Torchia DA (1999) Estimating the time scale of chemical exchange of proteins from measurements of transverse relaxation rates in solution. J Biomol NMR 14:369–372

Ishima R, Torchia DA (2000) Protein dynamics from NMR. Nat Struct Biol 7:740–743

Ishima R, Torchia DA (2006) Accuracy of optimized chemical exchange parameters derived by fitting CPMG dispersion profiles when $R_2^{0A} \neq R_2^{0B}$. J Biomol NMR 34:209–219

Ishima R, Freedberg DI, Wang YX, Louis JM, Torchia DA (1999) Flap opening and dimer-interface flexibility in the free and inhibitor- bound HIV protease, and their implications for function. Struct Fold Des 7:1047–1055

Iwahara J, Clore GM (2006) Detecting transient intermediates in macromolecular binding by paramagnetic NMR. Nature 440:1227–1230

Jen J (1978) Chemical exchange and NMR T2 relaxation—multisite case. J Magn Reson 30:111–128

Karplus M, Kuriyan J (2005) Molecular dynamics and protein function. Proc Natl Acad Sci USA 102:6679–6685

Korzhnev DM, Kay LE (2008) Probing invisible, low-populated States of protein molecules by relaxation dispersion NMR spectroscopy: an application to protein folding. Acc Chem Res 41:442–451

Korzhnev DM, Orekhov VY, Dahlquist FW, Kay LE (2003) Off-resonance R1rho relaxation outside of the fast exchange limit: an experimental study of a cavity mutant of T4 lysozyme. J Biomol NMR 26:39–48

Korzhnev DM, Salvatella X, Vendruscolo M, Di Nardo AA, Davidson AR, Dobson CM, Kay LE (2004) Low-populated folding intermediates of Fyn SH3 characterized by relaxation dispersion NMR. Nature 430:586–590

Korzhnev DM, Orekhov VY, Kay LE (2005) Off-resonance R(1rho) NMR studies of exchange dynamics in proteins with low spin-lock fields: an application to a Fyn SH3 domain. J Am Chem Soc 127:713–721

Korzhnev DM, Religa TL, Banachewicz W, Fersht AR, Kay LE (2010) A transient and low-populated protein-folding intermediate at atomic resolution. Science 329:1312–1316

Lange OF, Lakomek NA, Fares C, Schroder GF, Walter KF, Becker S, Meiler J, Grubmuller H, Griesinger C, de Groot BL (2008) Recognition dynamics up to microseconds revealed from an RDC-derived ubiquitin ensemble in solution. Science 320: 1471–1475

Lindorff-Larsen K, Best RB, Depristo MA, Dobson CM, Vendruscolo M (2005) Simultaneous determination of protein structure and dynamics. Nature 433:128–132

Luz Z, Meiboom S (1963) Nuclear magnetic resonance study of protolysis of trimethylammonium ion in aqueous solution-order of reaction with respect to solvent. J Chem Phys 39:366–370

McConnell HM (1958) Reaction rates by nuclear magnetic resonance. J Chem Phys 28:430–431

Miloushev VZ, Palmer AG 3rd (2005) R(1rho) relaxation for two-site chemical exchange: general approximations and some exact solutions. J Magn Reson 177:221–227

Mittermaier A, Kay LE (2006) New tools provide new insights in NMR studies of protein dynamics. Science 312:224–228

Palmer AG, Massi F (2006) Characterization of the dynamics of biomacromolecules using rotating-frame spin relaxation NMR spectroscopy. Chem Rev 106:1700–1719

Palmer AG, Williams J, McDermott A (1996) Nuclear magnetic resonance studies of biopolymer dynamics. J Phys Chem 100:13293–13310

Palmer AG, Kroenke CD, Loria JP (2001) NMR methods for quantifying microsecond-to-millisecond motions in biological macromolecules. Methods Enzymol 339:204–238

Palmer AG, Grey MJ, Wang C (2005) Solution NMR spin relaxation methods for characterizing chemical exchange in high-molecular-weight systems. Methods Enzymol 394:430–465

Skrynnikov NR, Dahlquist FW, Kay LE (2002) Reconstructing NMR spectra of "invisible" excited protein states using HSQC and HMQC experiments. J Am Chem Soc 124:12352–12360

Sprangers R, Kay LE (2007) Quantitative dynamic and binding studies of the 20S proteasome by NMR. Nature 445:618–622

Sugase K, Dyson HJ, Wright PE (2007) Mechanism of coupled folding and binding of an intrinsically disordered protein. Nature 447:1021–1024

Tang C, Schwieters CD, Clore GM (2007) Open-to-closed transition in apo maltose-binding protein observed by paramagnetic NMR. Nature 449:1078–1082

Trott O, Palmer AG 3rd (2002) R1rho relaxation outside of the fast-exchange limit. J Magn Reson 154:157–160